Electronic Supplementary Material (ESI) for RSC Advances.
This journal is © The Royal Society of Chemistry 2022

Electronic Supplementary Material (ESI) for Materials Chemistry Frontiers.
This journal is © the Partner Organisations 2022

Supplementary Material

Role of processing parameters in CVD grown crystalline monolayer $MoSe_2$

Girija Shankar Papanai[a,b], Krishna Rani Sahoo[c], Betsy Reshma G[b,d], Sarika Gupta[e]and Bipin Kumar Gupta[a,b,*]

[a]*Photonic Materials Metrology Sub Division, Advanced Materials and Device Metrology Division, CSIR-National Physical Laboratory, Dr. K. S. Krishnan Marg, New Delhi 110012, India*

[b]*Academy of Scientific and Innovative Research (AcSIR), Ghaziabad 201002, India*

[c]*Tata Institute of Fundamental Research - Hyderabad, Sy. No 36/P Serilingampally, Mandal, Gopanpally Village, Hyderabad 500046, India*

[d]*CSIR–Institute of Genomics and Integrative Biology, Mathura Road, New Delhi 110025, India*

[e]*Molecular Sciences Lab, National Institute of Immunology, Aruna Asaf Ali Marg, New Delhi 110067, India*

*E-mail:bipinbhu@yahoo.com

The contents of electronic supplementary material are listed as follows-

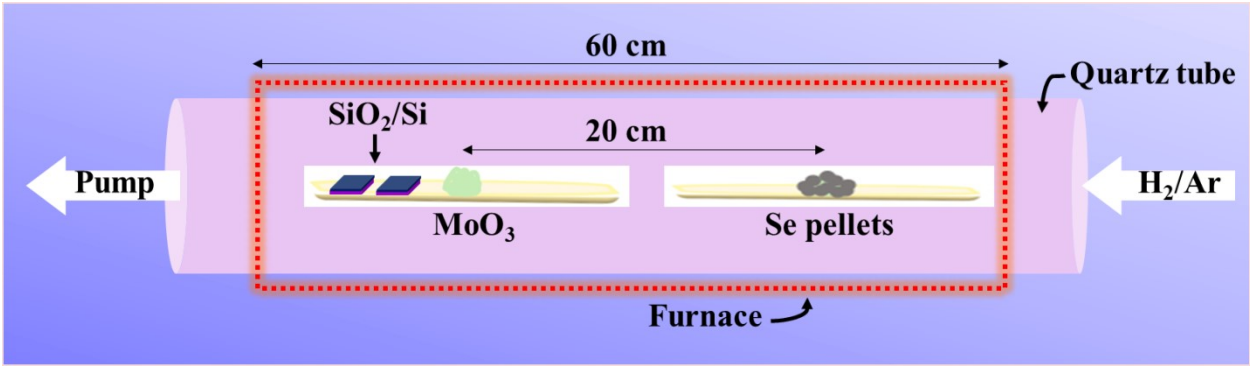

Figure S1. The schematic diagram of the CVD reaction chamber for growth of monolayer $MoSe_2$ flakes. The notations have their usual meaning.

S2. X-ray Diffraction of MoO_3 powder and Se pellets

XRD has been performed to check the quality of precursors prior to the synthesis of monolayer $MoSe_2$. Figure S2a shows the XRD pattern of MoO_3 powder, and the peak positions are well indexed with the orthorhombic MoO_3 [JCPDS card (Reference code: 00-005-0508)]. The XRD pattern of Se pellets is illustrated in Fig. S2b, and the peak positions are indexed with the hexagonal Se [JCPDS card (Reference code: 98-002-2251)].

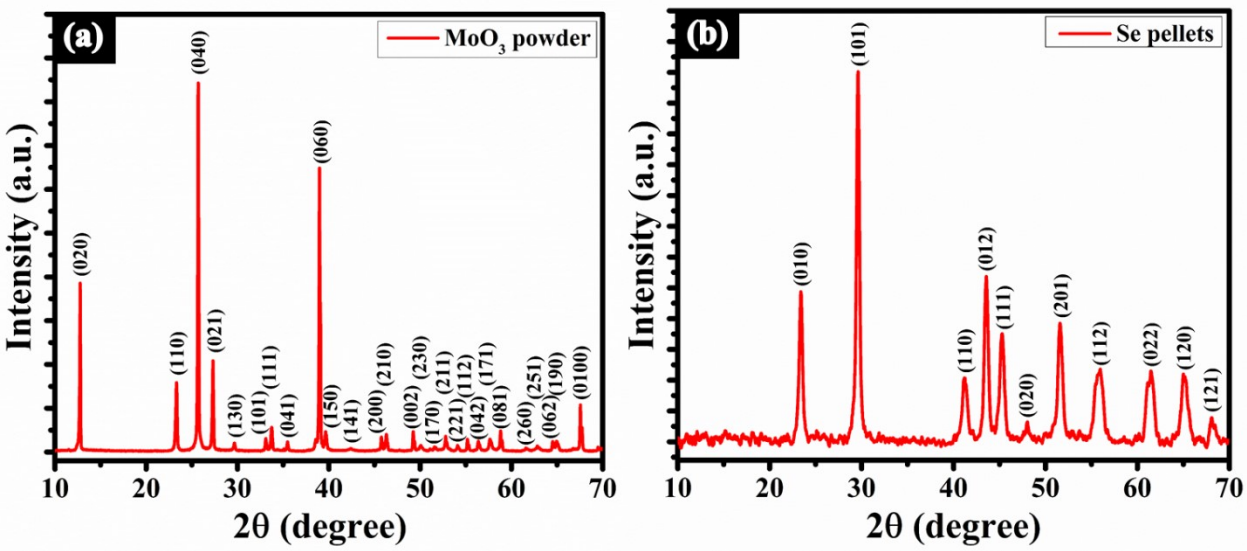

Figure S2. X-ray diffraction pattern of (a) MoO_3 powder and (b) Se pellets.

S3. AFM of monolayer $MoSe_2$ flakes over Si/SiO_2 substrate

AFM has been carried out to know the thickness of as-synthesized $MoSe_2$ flakes. Figure S3a shows the topographic image of $MoSe_2$ flakes at Si/SiO_2 substrate. The roughness parameters, *i.e.,* root mean square (image Rq) and average (image Ra) have been obtained to be ~5.8 and 1.8 nm, respectively. Figure S3b shows height profile along the green dotted line, where thickness has been found to be ~ 1.6 nm. On the other hand, the topographic image of ST shape of $MoSe_2$ flakes has been shown in Fig.S3c, having image Rq and image Ra values of ~7.4 and 3.2 nm. The height profile of ST shape along the green dotted line has been displayed in Fig.S3d, where the thickness has been observed to be ~ 2.8 nm. The variation in thickness of $MoSe_2$ flakes at two different locations suggests that the local changes occur in the precursor's ratio during growth. In earlier reports, the thickness of monolayer $MoSe_2$ is obtained in the range of 0.7 to 1 nm.[1–3] However, in the present work, obtained thickness has deviated from the monolayer thickness at both locations on same substrate. This deviation might be attributed to two reasons :(i) non-uniformity of the SiO_2 layer over Si substrate and (ii) trapped adsorbates between $MoSe_2$ flakes and substrate.

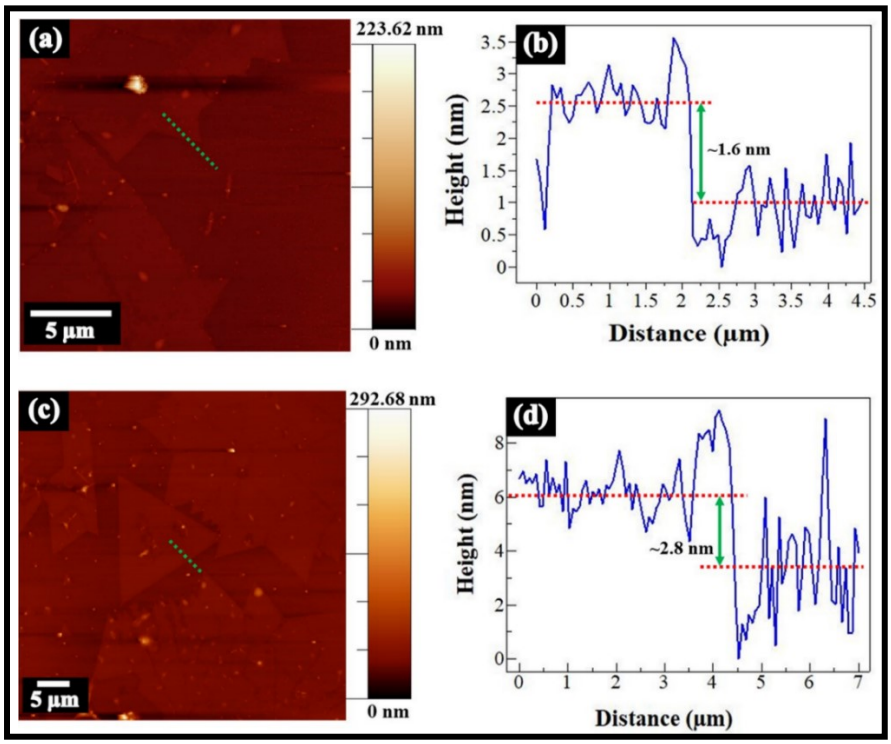

Figure S3. AFM topographic image of the as-synthesized $MoSe_2$ flakes on two different locations over Si substrate having SiO_2 thickness of 300 nm: (a) topographic image at the first location and (b) corresponding height profile across the green dotted line; (c) topographic

image at the second location of the same substrate and (d) height profile of ST shape along the green dotted line.

S4. Absorption spectrum on $MoSe_2$ flakes on the quartz substrate

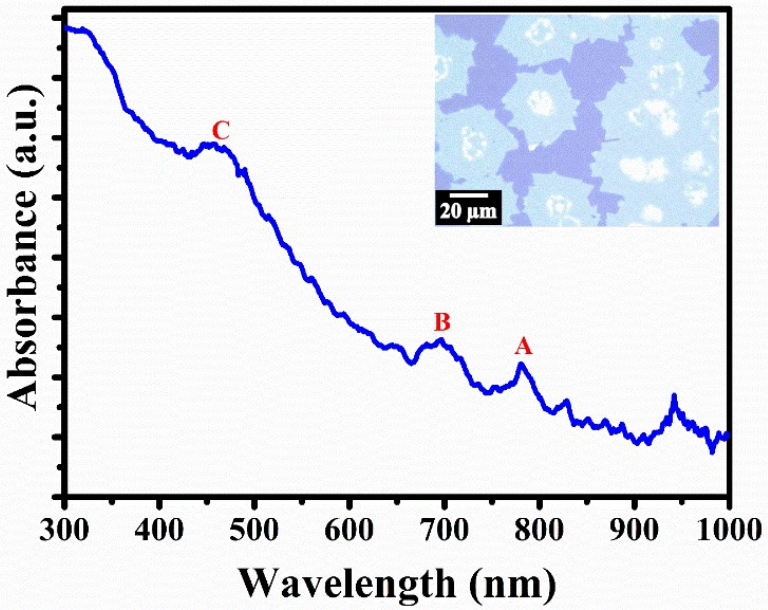

Figure S4. The absorption spectrum of monolayer $MoSe_2$ over quartz substrate and the inset shows the optical image of monolayer $MoSe_2$ flakes deposited on the quartz substrate.

Figure S4 displays the absorption spectrum of the monolayer $MoSe_2$ flakes over a quartz substrate. Inset shows the optical image of $MoSe_2$ flakes on the quartz substrate. One can observe the three excitonic states from Fig. S4, A exciton (~781 nm), B exciton (~696 nm), and C exciton (~457 nm), respectively. The A exciton state arises due to the direct excitonic transition at the K point in the *k*-space. The B exciton emerged from a spin-orbit split-off band, and C exciton originated because of nearly degenerate exciton states.[4]

S5. Excitonic peak energies in as-synthesized monolayer $MoSe_2$and as-obtained shapes

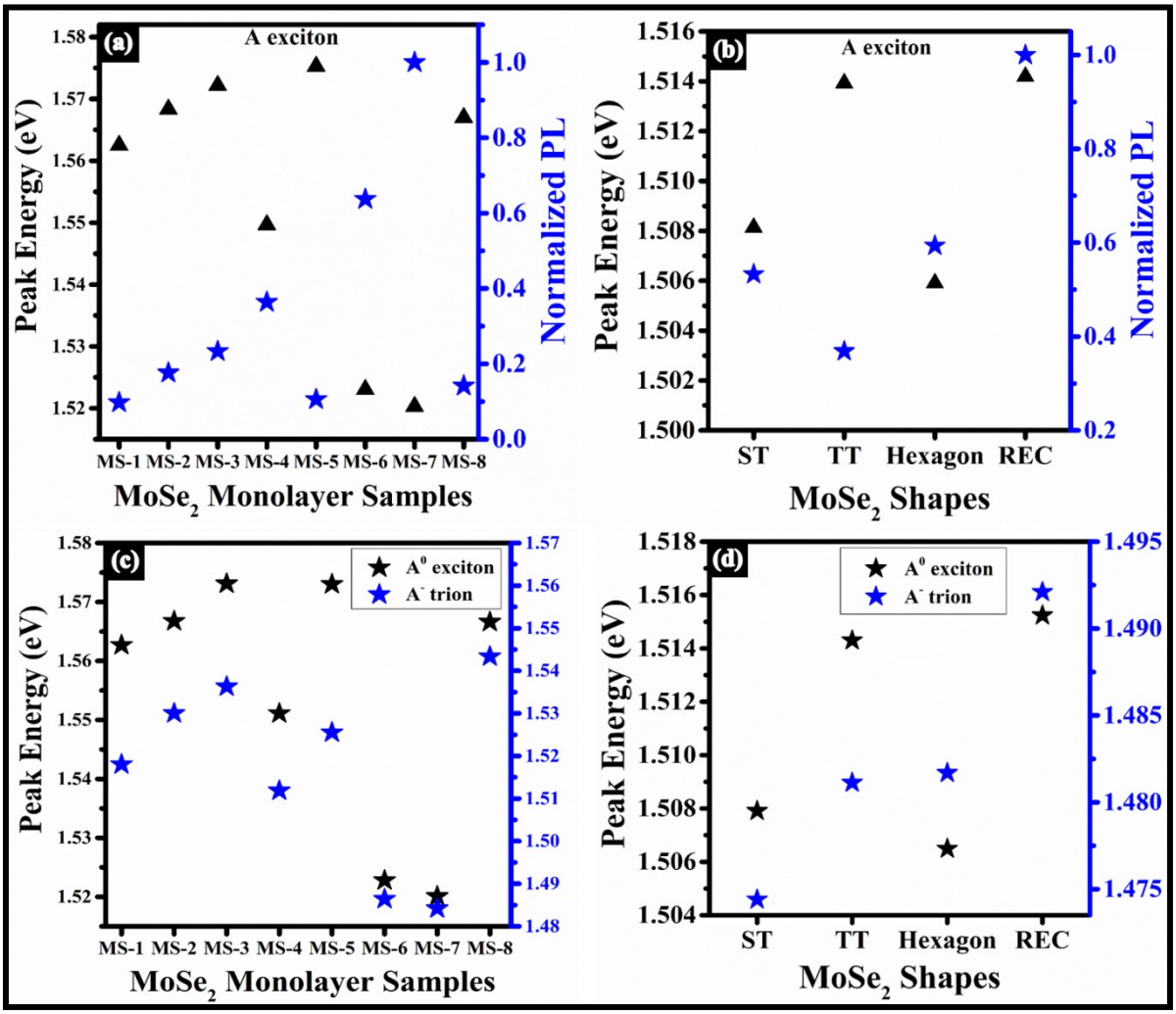

Figure S5. Peak energy of A exciton (left vertical axis) and normalized PL (right vertical axis) in (a) as-synthesized samples (MS-1 to MS-8) and (b) as-obtained shapes. Peak energy of A^0 exciton (left vertical axis) and A^- trion (right vertical axis): (c) as-synthesized samples and (d) as-obtained shapes.

S6. PL imaging of $MoSe_2$ flake having distorted hexagonal shape

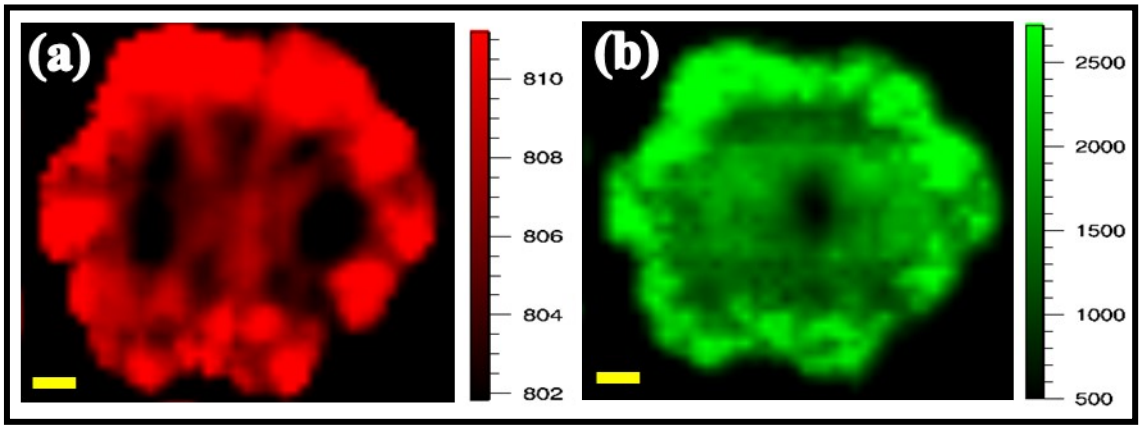

Figure S6. PL imaging of distorted hexagonal shape: (a) peak position and (b) peak intensity.

References:

1 J. C. Shaw, H. Zhou, Y. Chen, N. O. Weiss, Y. Liu, Y. Huang and X. Duan, Chemical vapor deposition growth of monolayer $MoSe_2$ nanosheets, *Nano Res.*, 2014, **7**, 511–517.

2 X. Lu, M. I. B. Utama, J. Lin, X. Gong, J. Zhang, Y. Zhao, S. T. Pantelides, J. Wang, Z. Dong, Z. Liu, W. Zhou and Q. Xiong, Large-Area Synthesis of Monolayer and Few-Layer $MoSe_2$ Films on SiO_2 Substrates, *Nano Lett.*, 2014, **14**, 2419–2425.

3 Y.-H. Chang, W. Zhang, Y. Zhu, Y. Han, J. Pu, J.-K. Chang, W.-T. Hsu, J.-K. Huang, C.-L. Hsu, M.-H. Chiu, T. Takenobu, H. Li, C.-I. Wu, W.-H. Chang, A. T. S. Wee and L.-J. Li, Monolayer $MoSe_2$ Grown by Chemical Vapor Deposition for Fast Photodetection, *ACS Nano*, 2014, **8**, 8582–8590.

4 D. Kozawa, R. Kumar, A. Carvalho, K. Kumar Amara, W. Zhao, S. Wang, M. Toh, R. M. Ribeiro, A. H. Castro Neto, K. Matsuda and G. Eda, Photocarrier relaxation pathway in two-dimensional semiconducting transition metal dichalcogenides, *Nat Commun*, 2014, **5**, 4543.